physical sciences forum

MDPI

Proceeding Paper

Entanglement Harvesting Between Unruh–DeWitt Detectors in de Sitter Spacetime †

Shagun Kaushal [1,*], Sanjay Pant [2] and Harsh Singh [3]

[1] Department of Physics, School of Advanced Sciences, Vellore Institute of Technology, Katpadi, Vellore 632014, India
[2] Department of Physics, School of Physical Sciences, DIT University Mussoorie-Diversion Road, Makkwala, Dehradun 248009, India; sanjay.pant@dituniversity.edu.in
[3] School of Computer Science Engineering and Information Systems, Vellore Institute of Technology, Katpadi, Vellore 632014, India; harsh.singh2023a@vitstudent.ac.in
* Correspondence: shagun.kaushal@vit.ac.in
† Presented at the 3rd International Online Conference on Universe, 4–6 March 2026; Available online: https://sciforum.net/event/IOCU2026.

Abstract

We investigate the harvesting of entanglement in de Sitter spacetime between two identical comoving Unruh–DeWitt detectors. The detectors interact locally with a complex scalar field after they are initially unentangled, creating an effective coupling. We examine massless minimally linked fields as well as conformally invariant fields, which behave differently in curved spacetime. We calculate negativity as a measure of entanglement and derive the reduced density matrix by tracing out field degrees of freedom. By contrasting both complex fields with the genuine scalar example, we discover that nonlinear couplings and complex fields improve entanglement robustness, enabling it to last over a larger parameter range, underscoring the significance of field structure.

Keywords: entanglement harvesting; Unruh–DeWitt detector; negativity

1. Introduction

Quantum entanglement is even more counterintuitive than normal quantum mechanical processes. Quantum entanglement is substantiated by robust experimental findings, including the violation of Bell inequalities, which classical theories predicated on local hidden variables fail to elucidate [1–3]. One of the things that makes entangled states different is that you cannot describe the Hilbert space that goes with them as a product of the pure states of subsystems, like [4,5] and the references within found. Quantum entanglement plays a crucial role in quantum physics and has been utilized in various modern applications, including the creation of advanced quantum teleportation devices and secure communication systems employing quantum cryptography [6–8].

Recent advancements have generated considerable interest in investigating quantum entanglement within the framework of relativistic quantum field theory [9–18]. A primary methodology entails the modelling of localized quantum systems interacting with quantum fields through particle detector frameworks. These studies focus on essential phenomena including entanglement dynamics, entanglement harvesting, and radiation emitted from entangled relativistic systems. Entanglement harvesting specifically offers a method to retrieve quantum correlations from the vacuum utilizing initially uncorrelated detectors. The Unruh–DeWitt detector model, initially created to study Unruh radiation and subsequently utilized for Hawking radiation, functions as a conventional instrument in this

Check for updates

Academic Editor: Gerald B. Cleaver

Published: 31 July 2026

Copyright: © 2026 by the authors. Licensee MDPI, Basel, Switzerland. This article is an open access article distributed under the terms and conditions of the Creative Commons Attribution (CC BY) license.

domain. In this study, we examine the circumstances that lead to the entanglement of such detectors through their interaction with a quantum field. Prior research demonstrates that the creation of detector entanglement is highly contingent on variables such as detector trajectories, spacetime geometry, environmental influences like thermal noise, and external disturbances including gravitational waves.

A significant amount of research has investigated entanglement harvesting through Unruh–DeWitt detectors interacting perturbatively with quantum fields, encompassing both inertial configurations in flat spacetime and non-inertial paths in curved backgrounds [19–30]. These studies encompass analyses of initially correlated detectors and examinations of non-perturbative effects. Comprehending these phenomena within an inflationary framework is particularly significant, as early-universe entanglement may influence cosmological observables, including correlation functions and the cosmic microwave background. As a result, entanglement in de Sitter spacetime has garnered considerable interest.

In this study, we examine entanglement harvesting between two identical, initially unentangled two-level detectors within cosmological de Sitter spacetime. The detectors follow paths that are both moving and coincident, and they interact with a complex scalar field. We examine both conformally coupled massless fields. Using leading-order perturbation theory, we make the reduced density matrix and find the logarithmic negativity to measure the harvested entanglement. We also look at how it depends on system parameters.

Throughout this work, we employ natural units $\hbar = c = 1$.

2. The Basic Setup

We now examine a complex scalar field (ϕ) connected to two Unruh–DeWitt detectors. For this composite system, the simplest interaction Hamiltonian is as follows:

$$\mathbf{H_I}(\tau_j) = \mathbf{g}\sum_j \chi(\tau_j)\mathbf{m}(\tau_j)\boldsymbol{\phi}^+(x(\tau_j))\boldsymbol{\phi}(x(\tau_j));\ j = A,\ B \tag{1}$$

where $\mathbf{g}$ is a dimensionless coupling constant, $\chi(\tau_j)$ is the switching function, and $\mathbf{m}(\tau_j)$ is the monopole moment operator of detector 'j' and $x(\tau_j)$ denotes its worldline parametrized by the proper time 'τ_j'. Here 'j' runs for both detectors, labelled as A and B. The quadratic coupling $\boldsymbol{\phi}^+\boldsymbol{\phi}$ is adopted because the field under consideration is a complex scalar field. This interaction is invariant under the global $\boldsymbol{U(1)}$ transformation $\boldsymbol{\phi} \to \mathbf{e}^{i\alpha}\boldsymbol{\phi}$, in contrast to a linear coupling to $\boldsymbol{\phi}$.

In the Heisenberg picture, we explicitly expand the monopole moment of the detectors as a function of the appropriate time as

$$\mathbf{m}(\tau_j) = \mathbf{e}^{i\omega_j\tau_j}\left|\mathbf{e_j}\right\rangle\left\langle\mathbf{g_j}\right| + \mathbf{e}^{-i\omega_j\tau_j}\left|\mathbf{g_j}\right\rangle\left\langle\mathbf{e_j}\right|; \tag{2}$$

$|\mathbf{g_j}\rangle$ and $|e_j\rangle$ in the above expression stand respectively for the ground and excited levels of the detectors. The oscillatory factors appearing in the detector response functions, shown in Equations (11) and (12), originate from the time dependence of the monopole operators in the interaction picture.

For simplicity, we imagine both detectors to be identical so that $\omega_j = \omega$ and $\chi_j = \chi$. And the switching function, as the Gaussian function, is defined as

$$\chi(\tau_j) = \mathbf{e}^{-\tau_j^2/2\sigma^2}. \tag{3}$$

The Gaussian switching function is chosen to model a smooth finite-time interaction between the detectors and the field. The parameter σ characterizes the duration of the interaction, while the overall interaction strength is controlled by the dimensionless coupling

https://doi.org/10.3390/psf2026014013

constant (g) appearing in Equation (1). The switching function is not normalized and is introduced solely to provide a smooth switching profile for the detector–field interaction.

We assume that both the field and detectors are in their ground state initially, so that their initial state is given as

$$|\,in\,\rangle = |\,0\;g_A\;g_B\,\rangle. \tag{4}$$

Being a perfect product state, it represents an unentanglement initially. The time evolution of this initial state in the interaction picture is given by

$$|out\;\rangle = U\,|in\;\rangle = \mathrm{T}\;e^{-i\int d\tau_j H_I(\tau_j)}|in\;\rangle, \tag{5}$$

where 'T' stands for time ordering. Using the perturbative expansion, we can rewrite U as

$$U = I + U^{(1)} + U^{(2)} + \ldots \tag{6}$$

where

$$U^{(1)} = -i\int_{-\infty}^{\infty} d\tau_j H_I(t(\tau_j)), \tag{7}$$

$$U^{(2)} = -\int_{-\infty}^{\infty} d\tau_i \int_{-\infty}^{\infty} d\tau_j' H_I(t(\tau_i)) H_I(t'(\tau_j')). \tag{8}$$

The density matrix of the initial state after time evolution is

$$\rho = |out\rangle\langle out| = \rho^{(0)} + \rho^{(1)} + \rho^{(2)} + O(g^3)\ldots \tag{9}$$

where $\rho^{(n)}$ denotes the contribution of order g^n. Throughout this work, we work in the weak coupling regime (g << 1), for which the leading nontrivial detector correlations arise at order g^2. Consequently, terms of order $O(g^3)$ and higher are neglected.

The reduced density matrix of the detectors is obtained by tracing over the field degrees of freedom,

$$\rho_{AB} = Tr_\phi(\rho)$$

Since the vacuum expectation value of the normal-ordered interaction vanishes, the leading nontrivial contribution arises at the second order. Using Wick's theorem, the field correlator appearing in the trace is $(iW(x,x'))^2$, where $(iW(x,x'))$ is the positive-frequency Wightman function of the complex scalar field.

The density matrix of two Unruh–DeWitt detectors is

$$\rho_{AB} = \begin{pmatrix} 1-X_{AA}-X_{BB} & 0 & 0 & M_{AB}^* \\ 0 & X_{AA} & X_{AB} & 0 \\ 0 & X_{AB} & X_{BB} & 0 \\ M_{AB} & 0 & 0 & 0 \end{pmatrix}. \tag{10}$$

in the basis $|\,g_A\;g_B\,\rangle$, $|\,g_A\;e_B\,\rangle$, $|\,e_A\;g_B\,\rangle$ and $|\,e_A\;e_B\,\rangle$, where the matrix elements read as

$$X_{IJ} = \int d\tau_I \int d\tau_J'\,\chi(\tau_I)\chi(\tau_J')\,e^{-i\,\omega(\tau_I-\tau_J')}\,(i\,W(x_I,x_J'))^2,\ (I,\,J = A,\,B) \tag{11}$$

$$M_{AB} = -\int d\tau_A \int d\tau_B\,\chi(\tau_A)\chi(\tau_B)\,e^{i\,\omega(\tau_A+\tau_B)}(i\,W(x_A,x_B))^2 \tag{12}$$

Here X_{AA} and X_{BB} correspond to the local excitations, X_{AB} characterizes detector–detector correlations induced by the field, and M_{AB} is the coherence term responsible for entanglement harvesting. In particular, for identical detectors, entanglement is harvested when the nonlocal coherence M_{AB} dominates over the local excitation probability X.

https://doi.org/10.3390/psf2026014013

$$\rho_{AB} = \begin{pmatrix} 1-2X & 0 & 0 & M^* \\ 0 & X & X_{AB} & 0 \\ 0 & X_{AB} & X & 0 \\ M & 0 & 0 & 0 \end{pmatrix}. \tag{13}$$

To evaluate the matrix elements X_{IJ} and M_{AB}, we require the Wightman function of a conformally coupled massless complex scalar field in de Sitter spacetime. We work in the spatially flat de Sitter metric

$$ds^2 = -d\tau^2 + e^{2H\tau}(dx^2 + dy^2 + dz^2)$$

where H is the Hubble parameter and τ denotes the proper time of the comoving observers. The two detectors follow comoving trajectories

$$x_A(\tau) = (\tau, x_A), \qquad x_B(\tau) = (\tau, x_B),$$

with fixed comoving separation $r = |x_A - x_B|$.

For the conformal vacuum state, the positive-frequency Wightman function is

$$iW(x_A, x_B') = \frac{H^2}{4\pi^2}(4\sinh^2(\frac{H}{2}((\tau_1 - \tau_2) - i\epsilon)) + e^{H(\tau_1+\tau_2)}r^2)^{-1}, \tag{14}$$

where $\epsilon > 0$ implements the standard positive-frequency '$i\epsilon$' prescription and regulates the coincidence singularity of the Wightman function. The principal branch associated with this prescription is assumed throughout. In all calculations, the limit $\epsilon \to 0^+$ is understood after regularization.

The quadratic detector–field interaction leads to the appearance of the squared Wightman function $(iW)^2$ **in Equations (11) and (12).** Although the Wightman function exhibits the usual short-distance singularity, the Gaussian switching function suppresses ultraviolet contributions and ensures that the detector response functions remain finite and well behaved. The regularized expressions employed in the numerical analysis follow Ref. [31].

3. Negativity of ρ_{AB}

3.1. Negativity

For mixed states, entanglement negativity is a good measure to quantify the entanglement of bipartite states [4,5,31,32]. It is defined as

$$N(\rho_{AB}) = \sum_i^n |\lambda_i|,$$

where λ_i are the negative eigenvalues of $\rho_{AB}^{T_A}$, where $\rho_{AB}^{T_A}$ is the partial transposed density matrix of ρ_{AB} with respect to the subspace of A.

To quantify the harvested entanglement, we compute the negativity of the detector density matrix. The partial transpose of Equation (13) is given by

$$\rho_{AB}^{T_A} = \begin{pmatrix} 1-2X & 0 & 0 & X_{AB} \\ 0 & X & M & 0 \\ 0 & M^* & X & 0 \\ X_{AB} & 0 & 0 & 0 \end{pmatrix}. \tag{15}$$

The eigenvalues of Equation (13) are given by

$$\lambda_{1,2} = \frac{1}{2}\left(1-2X \pm \sqrt{(1-2X)^2 + 4X_{AB}{}^2}\right), \quad \lambda_{3,4} = X \pm |M|$$

https://doi.org/10.3390/psf2026014013

The eigenvalues λ_1, λ_2, and λ_3 are non-negative, while $\lambda_4 = X - |M|$ becomes negative whenever

$$|M| \geq X, \tag{16}$$

According to the Peres–Horodecki positive partial transpose (PPT) criterion, a two-qubit state is entangled if and only if its partial transpose has at least one negative eigenvalue. Hence, the condition ($|M| > X$) determines the parameter regime in which entanglement harvesting occurs [30,31].

The negativity is defined as the absolute sum of the negative eigenvalues of $\rho_{AB}^{T_A}$. Since λ_4 is the only eigenvalue that can be negative, we obtain

$$\mathbf{N = max\{0, |M| - X\}}. \tag{17}$$

In the entangled region (($|M| > X$)), Equation (17) reduces to

$$\mathbf{N = |M| - X}$$

Since the eigenvalues depend only on the modulus ($|M|$), the above expression remains valid even when (M) is complex. Consequently, a positive value of (N) indicates that two initially separable detectors become entangled through their interaction with the quantum field. For two-qubit systems, the PPT criterion is both necessary and sufficient for entanglement, and therefore the negativity provides a complete characterization of entanglement in the present setup.

The local excitation probability **X** represents detector noise, whereas ***M*** characterizes nonlocal field-mediated correlations. Since $\mathbf{N = max\{0, |M| - X\}}$, entanglement harvesting occurs only when the nonlocal contribution exceeds the local noise contribution, even for super-horizon detector separations.

3.2. Transition Integrals

On substituting Equation (14) into Equations (2), (11) and (12), we obtain

$$\mathbf{X_{IJ} = \int d\tau_I \int d\tau_J{}'\, e^{-(\tau_I^2+\tau'^2_J)/2\sigma^2}\, e^{-i\,\omega(\tau_I-\tau_J{}')}\, (i\, W(x_I,x_J{}'))^2,}\ (I, J = A, B) \tag{18}$$

$$\mathbf{M_{AB} = -\int d\tau_A \int d\tau_B\, e^{-(\tau_A^2+\tau'^2_B)/2\sigma^2}\, e^{i\,\omega(\tau_A+\tau'_B)}\, (i\, W(x_A,x_B))^2.} \tag{19}$$

Evaluating further, we obtain the reformulated integrals as

$$\mathbf{X = \frac{H^2 g^2 h^2 e^{-\omega^2\sigma^2}}{96\,\pi^3} \int_0^\infty dk\, e^{-k^2}\, k^3\, \frac{\cosh\frac{k\pi}{h}}{\sinh\frac{k\pi}{h}} \left(1 - \frac{2h\omega\sigma}{\pi}\right).} \tag{20}$$

$$\mathbf{M = -\frac{H^2 g^2}{64\,\pi^{3/2}} \int_{-\infty}^{\infty} dx\, e^{-x^2+2i\omega\sigma x} \int_0^\infty dk\, e^{-k^2}\, k^3\, \frac{\sin\left(\frac{2kln a}{h}\right)\cosh\frac{2k\pi}{h}\left(\frac{h}{ln a} + 2ik\right)}{b(1+b^2h^2)\left(1 - e^{\frac{2\pi k}{h}}\right)}} \tag{21}$$

where $h = H\sigma$, $b = e^{hx}r/2\sigma$ and $\mathbf{a = bh + \sqrt{b^2h^2 + 1}}$. The multidimensional integrals in Equations (20) and (21) contain oscillatory exponential factors and are evaluated in the asymptotic parameter regime specified below. In this regime, the dominant contributions arise from the vicinity of the stationary points of the phase, allowing the use of the saddle-point (steepest-descent) approximation. Furthermore, the Gaussian switching function introduces exponential damping factors that suppress contributions from large integration variables, thereby improving the convergence properties of the integrals. Following

https://doi.org/10.3390/psf2026014013

Ref. [32], the asymptotic evaluation is performed using saddle-point techniques, and for brevity we refer the reader to Appendix A and Appendix B of Ref. [32] for the detailed derivation.

The analysis is conveniently expressed in terms of the dimensionless parameters $\boldsymbol{\omega\sigma}$, $h = H\sigma$, and $r/(2\sigma)$. The parameter $\boldsymbol{\omega\sigma}$ compares the detector energy gap $\boldsymbol{\omega}$ with the inverse interaction duration $\boldsymbol{\sigma}^{-1}$, and therefore measures the relative time scales of detector dynamics and switching. The parameter ($h = H\sigma$) compares the interaction duration with the de Sitter expansion time scale $\mathbf{H}^{-1}$. Finally, $r/(2\sigma)$ compares the detector separation with the interaction scale set by the switching function. Values $r/(2\sigma) > 1$ correspond to detectors separated by more than the effective interaction length associated with the switching duration. Throughout this work, we focus on the regime

$$\boldsymbol{\omega\sigma} \gg 1, \ \frac{\boldsymbol{\pi}}{\mathbf{h}} \gg 1, \text{ and } \frac{\mathbf{r}}{2\boldsymbol{\sigma}} > 1 \tag{22}$$

corresponding respectively to well-resolved detector transitions, interaction times much shorter than the cosmological expansion time scale, and spacelike separated detectors.

We calculated the entanglement negativity using Equation (17) after evaluating Equations (20) and (21) numerically. Figure 1 displays the behaviour of the same factors with respect to the dimensionless parameters '$r/2\sigma$' (detectors' separation), interaction duration '$H\sigma$', and '$\omega\sigma$' (energy gap) for different values of the coupling strength 'g'. It is evident that even at super-horizon separations ($r/2\sigma > 1$), the negativity can be nonzero, indicating ongoing nonlocal correlations in the conformal vacuum. Stronger coupling 'g' improves the entanglement harvesting, while increasing 'h' decreases entanglement caused by accumulated local noise. Additionally, the dependence on $\omega\sigma$ is non-monotonic: the negativity initially increases due to improved spectral overlap with field modes but decreases at higher values as short-wavelength modes contribute less to long-range correlations.

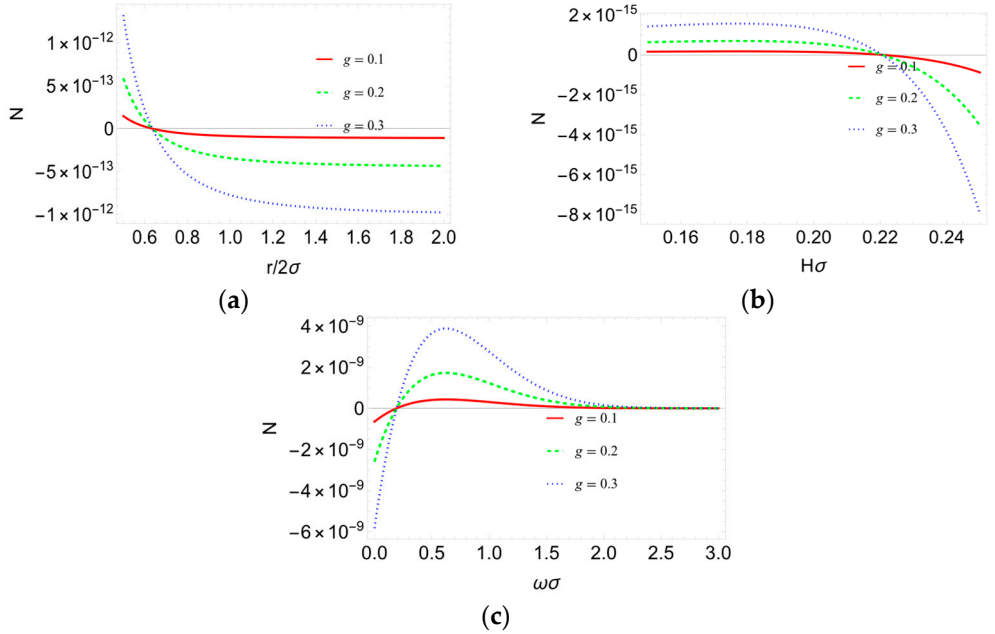


Figure 1. Variation in negativity (N) with respect to (**a**) detector separation ($r/2\sigma$), (**b**) interaction duration ($H\sigma$), and (**c**) energy gap ($\omega\sigma$) for different values of coupling constant (g).

4. Conclusions

In this study, we examined entanglement harvesting by two identical, comoving Unruh–DeWitt detectors in de Sitter spacetime, interacting through a conformally invariant

complex scalar field. We calculated negativity as an entanglement metric and analyzed its correlation with detector separation, energy gap, and interaction duration.

Our findings demonstrate that entanglement can be extracted even at super-horizon distances, underscoring the enduring nature of nonlocal correlations in the de Sitter vacuum. The amount of entanglement, on the other hand, depends on the energy gap and the length of the interaction. Larger values cause negativity to go down because of less spectral overlap and more local noise. The entanglement decreases smoothly as the separation or energy gap increases, without a sharp cutoff at the horizon scale. This is different from what was seen in earlier studies of real scalar fields with linear coupling, where the suppression was sudden.

These results show that entanglement harvesting is controlled by more than just the causal structure. It is also affected by the quantum nature of the field and the choice of coupling. The enduring nature of negativity reflects the foundational field theory, offering insights into the entanglement structure of quantum fields within curved spacetime.

Future directions include the extension of this analysis to diverse field types and couplings, the investigation of non-inertial detector trajectories, and the integration of decoherence effects. Studying the dynamics of decoherence between detectors may help us understand the quantum-to-classical transition in cosmological settings better. Extensions that include critical slowing down in systems with more than one detector are also good places to look for more research.

Author Contributions: Conceptualization, S.K.; methodology, S.K.; formal analysis, S.K.; investigation, S.K.; data curation, H.S.; writing—review and editing, H.S. and S.P. All authors have read and agreed to the published version of the manuscript.

Funding: This research received no external funding.

Institutional Review Board Statement: Not applicable.

Informed Consent Statement: Not applicable.

Data Availability Statement: The data presented in this study are available from the corresponding author upon reasonable request. No publicly archived datasets were generated or analyzed during the current study.

Conflicts of Interest: The authors declare no conflict of interest.

References

1. Einstein, B.P.; Rosen, N. Can Quantum-Mechanical Description of Physical Reality Be Considered Complete. *Phys. Rev.* **1935**, *47*, 777. [CrossRef]
2. Bell, S. On the Einstein-Podolsky-Rosen paradox. *Physics* **1964**, *1*, 195. [CrossRef]
3. Clauser, J.F.; Horne, M.A.; Shimony, A.; Holt, R.A. Proposed experiment to test local hidden-variable theories. *Phys. Rev. Lett.* **1969**, *23*, 880. [CrossRef]
4. Nielsen, M.A.; Chuang, I.L. *Quantum Computation and Information Theory*; Cambridge University Press: Cambridge, UK, 2010.
5. Horodecki, P. Separability criterion and inseparable mixed states with positive partial transposition. *Phys. Lett. A* **1997**, *232*, 333. [CrossRef]
6. Tittel, W.; Brendel, J.; Zbinden, H.; Gisin, N. Violation of Bell inequalities by photons more than 10 km apart. *Phys. Rev. Lett.* **1998**, *81*, 3563–3566. [CrossRef]
7. Salart, D.; Baas, A.; Branciard, C.; Gisin, N.; Zbinden, H. Testing spooky action at a distance. *Nature* **2008**, *454*, 861–864. [CrossRef] [PubMed]
8. Hotta, M. Quantum measurement information as a key to energy extraction from local vacuums. *Phys. Rev. D* **2008**, *78*, 045006. [CrossRef]
9. Fuentes-Schuller, I.; Mann, R.B. Alice falls into a black hole: Entanglement in non-inertial frames. *Phys. Rev. Lett.* **2005**, *95*, 120404. [CrossRef] [PubMed]
10. Reznik, B. Entanglement from the vacuum. *Found. Phys.* **2003**, *33*, 167–176. [CrossRef]

11. Martin-Martinez, E.; Smith, A.R.H.; Terno, D.R. Spacetime structure and vacuum entanglement. *Phys. Rev. D* **2016**, *93*, 044001. [CrossRef]
12. Fuentes, I.; Mann, R.B.; Martin-Martinez, E.; Moradi, S. Entanglement of Dirac fields in an expanding spacetime. *Phys. Rev. D* **2010**, *82*, 045030. [CrossRef]
13. Anastopoulos, C.; Hu, B.L.; Savvidou, K. Quantum field theory based quantum information: Measurements and correlations. *Ann. Phys.* **2023**, *450*, 169239. [CrossRef]
14. Lima, C.; Patterson, E.; Tjoa, E.; Mann, R.B. Unruh phenomena and thermalization for qudit detectors. *Phys. Rev. D* **2023**, *108*, 105020. [CrossRef]
15. Elghaayda, S.; Mansour, M. Entropy disorder and quantum correlations in two Unruh–DeWitt detectors uniformly accelerating and interacting with a massless scalar field. *Phys. Scr.* **2023**, *98*, 095254. [CrossRef]
16. Bhattacharya, S.; Chakrabortty, S.; Hoshino, H.; Kaushal, S. Background magnetic field and quantum correlations in the Schwinger effect. *Phys. Lett. B* **2020**, *811*, 135875. [CrossRef]
17. Kaushal, S. Fermionic entanglement in the presence of background electric and magnetic fields. *Eur. Phys. J. C* **2025**, *85*, 75. [CrossRef]
18. Kaushal, S. Schwinger effect and a uniformly accelerated observer. *Eur. Phys. J. C* **2022**, *82*, 872. [CrossRef]
19. Zhang, J.; Yu, H. Entanglement harvesting for Unruh-DeWitt detectors in circular motion. *Phys. Rev. D* **2020**, *102*, 065013. [CrossRef]
20. Henderson, L.J.; Hennigar, R.A.; Mann, R.B.; Smith, A.R.H.; Zhang, J. Harvesting Entanglement from the Black Hole Vacuum. *Class. Quant. Grav.* **2018**, *35*, 21LT02. [CrossRef]
21. Wu, D.; Tang, S.C.; Shi, Y. Birth and death of entanglement between two accelerating Unruh-DeWitt detectors coupled with a scalar field. *J. High Energy Phys.* **2023**, *2023*, 37. [CrossRef]
22. Martin-Martinez, E.; Menicucci, N.C. Cosmological quantum entanglement. *Class. Quant. Grav.* **2012**, *29*, 224003. [CrossRef]
23. Tjoa, E.; Mann, R.B. Unruh-DeWitt detector in dimensionally-reduced static spherically symmetric spacetimes. *J. High Energy Phys.* **2022**, *2022*, 14. [CrossRef]
24. Bhattacharya, D.; Gallock-Yoshimura, K.; Henderson, L.J.; Mann, R.B. Extraction of entanglement from quantum fields with entangled particle detectors. *Phys. Rev. D* **2023**, *107*, 105008. [CrossRef]
25. Dhanuka, A.; Lochan, K. Unruh–DeWitt probe of late time revival of quantum correlations in Friedmann spacetimes. *Phys. Rev. D* **2022**, *106*, 125006. [CrossRef]
26. Maeso-García, H.; Polo-Gómez, J.; Martín-Martínez, E. How measuring a quantum field affects entanglement harvesting. *Phys. Rev. D* **2023**, *107*, 045011. [CrossRef]
27. Martin-Martinez, E.; Sanders, B.C. Precise space–time positioning for entanglement harvesting. *New J. Phys.* **2016**, *18*, 043031. [CrossRef]
28. Barman, D.; Barman, S.; Majhi, B.R. Entanglement harvesting between two inertial Unruh-DeWitt detectors from nonvacuum quantum fluctuations. *Phys. Rev. D* **2022**, *106*, 045005. [CrossRef]
29. Nambu, Y. Entanglement Structure in Expanding Universes. *Entropy* **2013**, *15*, 1847–1874. [CrossRef]
30. Kukita, S.; Nambu, Y. Harvesting large scale entanglement in de Sitter space with multiple detectors. *Entropy* **2017**, *19*, 449. [CrossRef]
31. Vidal, G.; Werner, R.F. Computable measure of entanglement. *Phys. Rev. A* **2002**, *65*, 032314. [CrossRef]
32. Kaushal, S.; Bhattacharya, S. Entanglement generation between Unruh-DeWitt detectors in the de Sitter spacetime—Analysis with complex scalar fields. *Ann. Phys.* **2025**, *482*, 170235. [CrossRef]

Disclaimer/Publisher's Note: The statements, opinions and data contained in all publications are solely those of the individual author(s) and contributor(s) and not of MDPI and/or the editor(s). MDPI and/or the editor(s) disclaim responsibility for any injury to people or property resulting from any ideas, methods, instructions or products referred to in the content.